

Dynamic Cooper Pair Splitter

Fredrik Brange,¹ Kacper Prech,^{1,2} and Christian Flindt¹

¹*Department of Applied Physics, Aalto University, 00076 Aalto, Finland*

²*School of Physics and Astronomy, University of Glasgow, Glasgow, G12 8QQ, UK*

Cooper pair splitters are promising candidates for generating spin-entangled electrons. However, the splitting of Cooper pairs is a random and noisy process, which hinders further synchronized operations on the entangled electrons. To circumvent this problem, we here propose and analyze a dynamic Cooper pair splitter that produces a noiseless and regular flow of spin-entangled electrons. The Cooper pair splitter is based on a superconductor coupled to quantum dots, whose energy levels are tuned in and out of resonance to control the splitting process. We identify the optimal operating conditions for which exactly one Cooper pair is split per period of the external drive and the flow of entangled electrons becomes noiseless. To characterize the regularity of the Cooper pair splitter in the time domain, we analyze the $g^{(2)}$ -function of the output currents and the distribution of waiting times between split Cooper pairs. Our proposal is feasible using current technology, and it paves the way for dynamic quantum information processing with spin-entangled electrons.

Introduction.— Superconductors are natural sources of entangled particles [1]. By splitting the Cooper pairs in a superconductor into different normal-state leads, spin-entanglement between spatially separated electrons can be achieved [2, 3]. Cooper pair splitters have been realized in several types of solid-state architectures [4–19], for instance using quantum dots [6, 9, 11], carbon nanotubes [7], or graphene [15, 16, 18]. Experimentally, the splitting process has been observed by measuring the non-local conductance or the noise [8, 12] and recently using single-electron detectors [19]. However, with static voltages, the generation of spin-entangled electrons is a random and noisy process, which offers little control over the regularity and the timing of the Cooper pair splitting.

In parallel with these developments, dynamic single-electron emitters have emerged as accurate sources of noiseless currents [20–28]. By applying periodic gate or bias voltages to a nano-scale structure, such as a quantum dot [24, 25, 27, 28], a mesoscopic capacitor [20, 22], or an ohmic contact [23, 26], single electrons can be periodically emitted into a ballistic conductor, leading to an electric current which is given simply by the driving frequency times the charge of an electron [29]. So far, these efforts have mainly focused on dynamic sources that emit a single electron per cycle. However, one may envision other types of sources that emit more complex quantum states, for example with several entangled particles.

In this Letter, we propose and analyze a dynamic Cooper pair splitter that can deliver a noiseless and regular stream of spin-entangled electrons. Specifically, we show how the splitting of Cooper pairs can be controlled by applying time-dependent gate voltages to two quantum dots that are connected to a superconductor. We evaluate the average current and the fluctuations in the output leads and identify the optimal operating conditions for the dynamic Cooper pair splitter to produce a noiseless and regular current. Our proposal seems feasible in the light of recent experimental advances, and it may be realized using current technology.

Dynamic Cooper pair splitter.— Figure 1(a) shows our dynamic Cooper pair splitter consisting of a superconductor coupled to two single-level quantum dots. Cooper pairs from the superconductor are split between the dots due to strong on-site Coulomb interactions, which prevent each dot from being doubly occupied. Electrons on the dots are collected in separate normal-metal drain

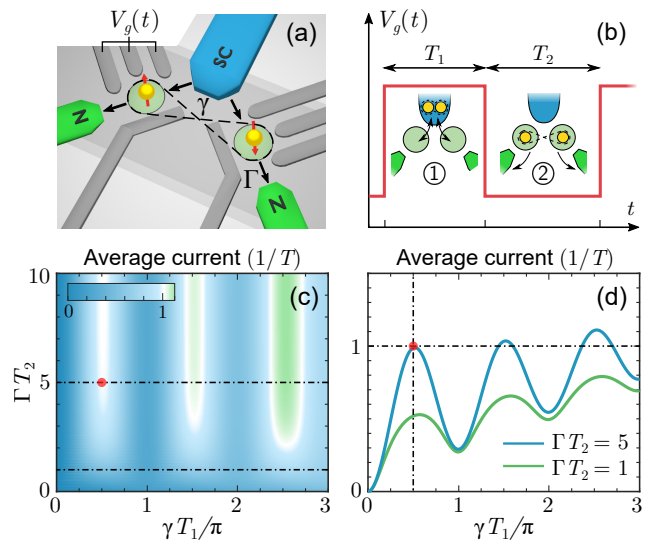


FIG. 1. Dynamic Cooper pair splitter. (a) The Cooper pair splitter consists of two quantum dots (light green) coupled to a superconductor (blue) and two normal-metal drains (green). The splitting of Cooper pairs is controlled with the time-dependent gate voltage, $V_g(t)$. (b) In phase ① of the periodic driving protocol, Cooper pair splitting is tuned into resonance for the time T_1 , so that a split Cooper pair tunnels into the dots (see insets). In phase ②, Cooper pair splitting is off resonance for the time T_2 , and the electrons may escape via the drains. (c,d) Average current in the drains as a function of T_1 and T_2 for $\Gamma = 0.1\gamma$, $\kappa = \gamma$, $\delta = 100\kappa$, with $\varepsilon = 0$ in phase ① and $\varepsilon = 100\gamma$ in phase ② (see main text for definitions). For the sweet-spot conditions, $\gamma T_1 = \pi/2$, and $\Gamma T_2 = 5$, shown with a red dot, one Cooper pair is split per period of the drive.

electrodes. Importantly for our proposal, we dynamically control the splitting of Cooper pairs using a time-dependent gate voltage $V_g(t)$ as we explain below.

For a large superconducting gap, the coherent dynamics of the dots due to the coupling to the superconductor can be described by the effective Hamiltonian [30–33]

$$\hat{H}(t) = \sum_{\ell\sigma} \epsilon_\ell(t) \hat{d}_{\ell\sigma}^\dagger \hat{d}_{\ell\sigma} - \left(\gamma \hat{d}_S^\dagger + \sum_{\sigma} \kappa \hat{d}_{L\sigma}^\dagger \hat{d}_{R\sigma} + \text{H.c.} \right), \quad (1)$$

where $\hat{d}_{\ell\sigma}^\dagger$ creates an electron with spin $\sigma = \uparrow, \downarrow$ in dot $\ell = L, R$, while $\hat{d}_S^\dagger \equiv (\hat{d}_{L\downarrow}^\dagger \hat{d}_{R\uparrow}^\dagger - \hat{d}_{L\uparrow}^\dagger \hat{d}_{R\downarrow}^\dagger)/\sqrt{2}$ creates a two-electron spin-singlet state, which is delocalized across the two dots. Here, the (real) amplitudes for Cooper pair splitting and elastic cotunneling are denoted by γ and κ , respectively, and $\epsilon_\ell(t)$ is the time-dependent energy level of each dot, which we tune by external gates to control the splitting of Cooper pairs and elastic cotunneling between the dots. Elastic cotunneling occurs mainly, when the dot levels are aligned and the detuning $\delta = \epsilon_L - \epsilon_R$ vanishes. Similarly, Cooper pair splitting is on resonance, when the doubly occupied dots have the same energy as the empty dots and the sum $\varepsilon = \epsilon_L + \epsilon_R$ vanishes. In general, Cooper pair splitting and elastic cotunneling lead to coherent oscillations with angular frequencies $\omega_\gamma = \sqrt{4\gamma^2 + \varepsilon^2}$ and $\omega_\kappa = \sqrt{4\kappa^2 + \delta^2}$, respectively, and both processes are suppressed as $\gamma^2/(\gamma^2 + \varepsilon^2/4)$ and $\kappa^2/(\kappa^2 + \delta^2/4)$ as we move away from the resonances. These suppression factors provide us with efficient experimental knobs to control the two types of processes. Thus, in the following, we consider the periodic driving protocol in Fig. 1(b), where Cooper pair splitting is tuned in ($\varepsilon = 0$) and out ($\varepsilon \gg \gamma$) of resonance, while elastic cotunneling is kept off resonance ($\delta \gg \kappa$). The duration of each phase is denoted by T_j , $j = 1, 2$, with \hat{H}_j being the corresponding Hamiltonian, and $T = T_1 + T_2$ is the period of the drive.

With large negative voltages on the drains, the time-evolution is governed by the Lindblad equation [34, 35]

$$\frac{d}{dt} \hat{\rho}(t) = \mathcal{L}_j \hat{\rho}(t) = -\frac{i}{\hbar} [\hat{H}_j, \hat{\rho}(t)] + \mathcal{D} \hat{\rho}(t) \quad (2)$$

for each of the phases with Liouvillian \mathcal{L}_j , $j = 1, 2$, and $\hat{\rho}(t)$ is the density matrix of the dots, while the dissipator

$$\mathcal{D} \hat{\rho}(t) = \Gamma \sum_{\sigma, \ell=L, R} \left(\mathcal{J}_{\ell\sigma} \hat{\rho}(t) - \frac{1}{2} \{ \hat{\rho}(t), \hat{d}_{\ell\sigma}^\dagger \hat{d}_{\ell\sigma} \} \right) \quad (3)$$

describes the coupling to the drains. The jump operators $\mathcal{J}_{\ell\sigma} \hat{\rho}(t) \equiv \hat{d}_{\ell\sigma} \hat{\rho}(t) \hat{d}_{\ell\sigma}^\dagger$ describe the tunneling of single electrons to the drains with the same rate Γ to keep the discussion simple, and from hereon we take $\hbar, e = 1$.

Driving protocol.— We first consider our driving protocol in the weak coupling limit, $\Gamma \ll \gamma, \kappa$, suppressing elastic cotunneling using the off-resonance condition $\delta \gg \kappa$. The protocol is designed as follows: In the first

phase (①), Cooper pair splitting is tuned into resonance ($\varepsilon = 0$) for the time T_1 . Ideally, during this phase, a Cooper pair is split between the dots, and we refer to T_1 as the loading time. In the second phase (②), Cooper pair splitting is turned off resonance ($\varepsilon \gg \gamma$) for the unloading time T_2 , allowing the split Cooper pair to leave the dots via the drains. We now consider the current in the drains to optimize the loading and unloading times.

Figure 1(c,d) shows the average current for the periodic driving protocol obtained using a method described below. The current oscillates as a function of the loading time T_1 due to the coherent oscillations induced by Cooper pair splitting in the first phase. By contrast, the current increases monotonously as a function of T_2 until it saturates for $\Gamma T_2 \gtrsim 5$, reflecting that the unloading time is sufficiently long for the electrons to leave the dots. In this regime, the average current [the blue curve in Fig. 1(d)] can be captured by the simple expression

$$I = \frac{1}{T} \left(\sin^2(\gamma T_1) + \frac{1}{2} [\Gamma T_1 + (1 - e^{-\Gamma T_1}) \cos(2\gamma T_1)] \right), \quad (4)$$

where the first term stems from the coherent oscillations for very small drain couplings, $\Gamma T_1 \ll 1$. Corresponding to this term, exactly one Cooper pair is split per period, if $\gamma T_1 = \pi(1/2 + m)$ for integer m . For finite couplings, the second term describes an unwanted leakage current during the first phase, which can be minimized by choosing a short loading time, $\Gamma T_1 \ll 1$. Thus, we find the sweet-spot conditions $\gamma T_1 = \pi/2 \gg \Gamma T_1$ and $\Gamma T_2 \simeq 5$ shown with a red dot in Fig. 1(c,d), where on average one Cooper pair is split per period of the drive.

Fluctuations.— We now proceed with a refined analysis of the Cooper pair splitter by investigating the auto and cross-correlations of the output currents. To this end, we use techniques from full counting statistics and decompose the density matrix as $\hat{\rho}(t) = \sum_{\mathbf{n}} \hat{\rho}(\mathbf{n}, t)$, so that $P(\mathbf{n}, t) = \text{tr} \{ \hat{\rho}(\mathbf{n}, t) \}$ is the joint probability that $\mathbf{n} = (n_L, n_R)$ electrons have been collected in the drains during the time span $[0, t]$ [36, 37]. The Lindblad equation renders a hierarchy of coupled equations for $\hat{\rho}(\mathbf{n}, t)$, which are decoupled by introducing counting fields $\boldsymbol{\chi} = (\chi_L, \chi_R)$ via the transformation $\hat{\rho}(\boldsymbol{\chi}, t) = \sum_{\mathbf{n}} \hat{\rho}(\mathbf{n}, t) e^{i\mathbf{n} \cdot \boldsymbol{\chi}}$. We thereby obtain a generalized master equation for $\hat{\rho}(\boldsymbol{\chi}, t)$ with χ -dependent Liouvillians $\mathcal{L}_j(\boldsymbol{\chi})$, obtained by substituting $\mathcal{J}_{\ell\sigma} \rightarrow e^{i\chi_\ell} \mathcal{J}_{\ell\sigma}$ in Eq. (3) [33].

The moment generating function for the number of emitted electrons after N periods now reads [38–40]

$$M(\boldsymbol{\chi}, N) = \text{tr} \{ \hat{\rho}(\boldsymbol{\chi}, NT) \} = \text{tr} \{ [\mathcal{U}(\boldsymbol{\chi}, T, 0)]^N \hat{\rho}_C(0) \}, \quad (5)$$

where the evolution operator for a time-dependent Liouvillian is given by a time-ordered exponential as $\mathcal{U}(\boldsymbol{\chi}, t, t_0) = \mathcal{T} \{ \exp[\int_{t_0}^t \mathcal{L}(\boldsymbol{\chi}, t') dt'] \}$, which we can explicitly evaluate for our piecewise constant protocol, and the cyclic state is determined by the eigenproblem $\mathcal{U}(\mathbf{0}, T + t, t) \hat{\rho}_C(t) = \hat{\rho}_C(t)$. The cumulants of the currents are

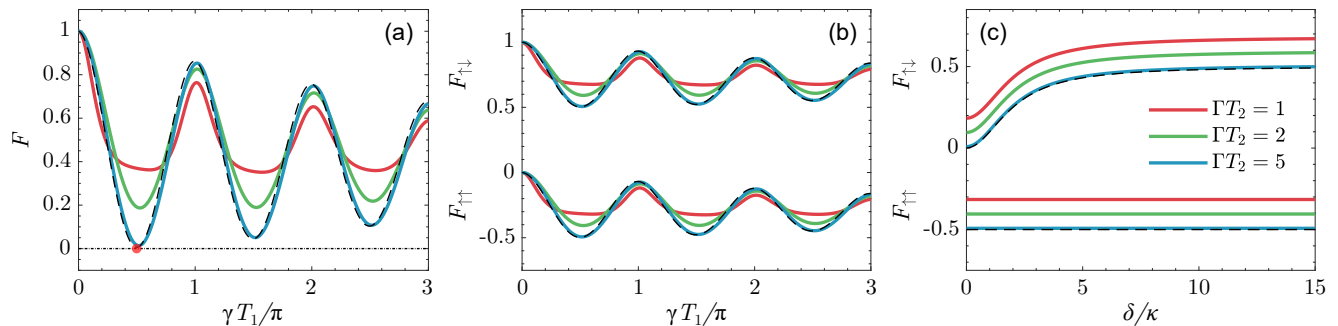


FIG. 2. Noise and spin correlations. (a) Fano factor as a function of the loading time T_1 for $\Gamma = 0.1\gamma$, $\gamma = \kappa$, $\delta = 100\kappa$, with $\varepsilon = 0$ in phase ①, and $\varepsilon = 100\gamma$ in phase ②. (b) Fano factors of the spin cross-correlations as a function of T_1 for the same settings as in panel (a). (c) Fano factors of the spin-correlations as functions of δ with $\gamma T_1 = \pi/2$ and otherwise same parameters as in panel (a). The dashed lines in panels (a), (b), and (c) are given by Eqs. (6), (7), and (8), respectively.

then given by derivatives of the cumulant generating function $F(\boldsymbol{\chi}) = \lim_{N \rightarrow \infty} \ln[M(\boldsymbol{\chi}, N)]/NT$ with respect to the counting fields as $\langle\langle I_\ell^k \rangle\rangle = \partial_{i\chi_L}^k \partial_{i\chi_R}^l F(\boldsymbol{\chi})|_{\boldsymbol{\chi}=0}$. With these definitions at hand, we can calculate the average currents and their correlations using the methods developed in Refs. [41–43] and in some regimes obtain simple expressions as those in Eq. (4) and Eq. (6) below.

Noise and Fano factor.— Figure 2(a) shows the Fano factor, $F_\ell = \langle\langle I_\ell^2 \rangle\rangle / \langle\langle I_\ell \rangle\rangle^2$, $\ell = L, R$, of the noise in the drain electrodes, which for regular transport is suppressed below the Poisson value of one. Here, the Fano factor oscillates as a function of the loading time T_1 , similarly to the average current in Fig. 1(c,d), and for long unloading times, $\Gamma T_2 \gg 1$, we find the simple expression

$$F = 1 - TI + \frac{2\Gamma T_1(1 + \Gamma T_1) + e^{-2\Gamma T_1} - 1}{8TI}, \quad (6)$$

corresponding to the dashed line in Fig. 2(a). For weak drain couplings, $\Gamma T_1 \ll 1$, the Fano factor reduces to $F = \cos^2(\gamma T_1)$, reflecting the coherent oscillations in the first phase. For larger couplings, the leakage current in the loading phase generates noise since more than one Cooper pair may be split during each period. Thus, we may minimize the noise by choosing $\gamma T_1 = \pi/2$ together with a long unloading time, $\Gamma T_2 \gg 1$, corresponding to the red dot in Fig. 2(a). (For short unloading times, the dots may not be emptied after each period, leading to cycle-missing events that generate noise.) Thus, the device produces N split Cooper pairs after N periods, when operated at the sweet spot in Figs. 1 and 2, and it is noiseless in contrast to a static Cooper pair splitter.

Spin-current correlations.— Next, we consider the cross-correlations between the drain currents and, in particular, between the spin currents in each drain, which play an important role for detecting the entanglement of the split Cooper pairs [44–47]. It is straightforward to include spin-dependent counting fields in Eq. (5), and in Fig. 2(b) we show the resulting cross-correlations of the spin-currents, $F_{\sigma\sigma'} = \langle\langle I_{L\sigma} I_{R\sigma'} \rangle\rangle / \sqrt{\langle\langle I_{L\sigma} \rangle\rangle \langle\langle I_{R\sigma'} \rangle\rangle}$, as

functions of the loading time T_1 . The anti-parallel spin currents are positively correlated, while parallel spins exhibit negative correlations, as expected for a split Cooper pair in a spin-singlet state. For long unloading times, $\Gamma T_2 \gg 1$, we find that the spin correlations Fig. 2(b) can be related to the Fano factor of the charge currents as

$$F_{\uparrow\downarrow} = 1 + F_{\uparrow\uparrow} = \frac{1}{2}(F + 1), \quad (7)$$

making it possible to determine the spin correlations from noise measurements of the charge currents in the drains.

In Fig. 2(c), we consider the spin-correlations as we tune elastic cotunneling into resonance. The negative correlations for parallel spins are essentially unchanged as elastic cotunneling is included. On the other hand, the positive correlations for anti-parallel spins are gradually washed out by elastic cotunneling. To better understand the effect of cotunneling, we consider a short loading time, $\Gamma T_1 \ll 1$, so that the leakage current is negligible during the first phase, and a long unloading time, $\Gamma T_2 \gg 1$, ensuring that at most one Cooper pair is split per period. Each uncorrelated period may then produce one of five outcomes; either no Cooper pair is split and no electrons reach the drain, or one Cooper pair is split and the two electrons tunnel into either of the two drains. We then approximate the generating function as

$$M(\boldsymbol{\chi}, N) \simeq \left[1 - p + \frac{pq}{2} \left(e^{i(\chi_\uparrow^L + \chi_\downarrow^L)} + e^{i(\chi_\uparrow^R + \chi_\downarrow^R)} \right) + \frac{p(1-q)}{2} \left(e^{i(\chi_\uparrow^L + \chi_\uparrow^R)} + e^{i(\chi_\downarrow^L + \chi_\downarrow^R)} \right) \right]^N, \quad (8)$$

where $p = \sin^2(\omega_\gamma T_1/2)\gamma^2/(\gamma^2 + \varepsilon^2/4)$ is the probability that a Cooper pair is split in the first phase, and $q = \frac{1}{2}\kappa^2/[\kappa^2 + (\Gamma^2 + \delta^2)/4]$ is the probability that the electrons leave via the same drain in the second phase due to elastic cotunneling. In Fig. 2(c), we show calculations of the spin-correlations based on this approximation and find good agreement with the exact results. Furthermore, we

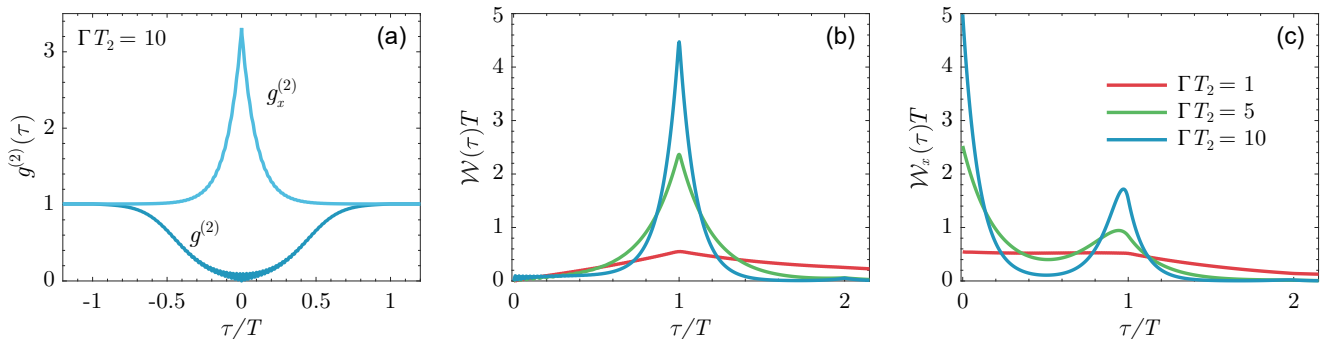


FIG. 3. Time-domain observables. (a) Auto and cross-correlations ($g_x^{(2)}$) of the drain currents. (b) Distributions of waiting times between electrons tunneling into the same drain. (c) Distributions of waiting times between electrons tunneling into different drains. Parameters are $\gamma T_1 = \pi/2$, $\Gamma = 0.05\gamma$, $\kappa = \gamma$, $\delta = 20\kappa$ with $\varepsilon = 0$ in phase ① and $\varepsilon = 20\gamma$ in phase ②.

find $F_{\uparrow\uparrow} = -p/2$ and $F_{\uparrow\downarrow} = 1 - p/2 - q$, which shows that, in this regime, $F_{\uparrow\uparrow}$ and $F_{\uparrow\downarrow}$ are sufficient to determine p and q and thus fully characterize the noise statistics.

Time-domain analysis.— Above, we focused on conventional low-frequency measurements of the current and the noise. However, as in the recent experiment of Ref. [19], additional information can be obtained by analyzing the fluctuations in the time-domain. (For example, a device that splits two Cooper pairs every second period produces the same low-frequency noise as one that splits one Cooper pair per period.) To this end, we consider the $g^{(2)}$ -function of the drain currents [48, 49], defined as

$$g_{\ell\ell'}^{(2)}(\tau) = \int_0^T dt_0 \frac{\langle\langle \mathcal{J}_\ell \mathcal{U}(\mathbf{0}, t_0 + \tau, t_0) \mathcal{J}_{\ell'} \rangle\rangle_{t_0}}{\langle\langle \mathcal{J}_\ell \rangle\rangle_{t_0 + \tau} \langle\langle \mathcal{J}_{\ell'} \rangle\rangle_{t_0}} P_{\ell'}(t_0) \quad (9)$$

for a periodic drive. Here, the probability density for the time that a tunneling event occurs reads $P_\ell(t) = \langle\langle \mathcal{J}_\ell \rangle\rangle_t / \int_0^T d\tau \langle\langle \mathcal{J}_\ell \rangle\rangle_\tau$, and $\langle\langle \mathcal{A} \rangle\rangle_t = \text{tr}\{\mathcal{A} \hat{\rho}_C(t)\}$ is the expectation value of \mathcal{A} . In this definition, the correlations due to the periodic drive have been factored out.

Figure 3(a) shows the $g^{(2)}$ -functions for the auto and the cross-correlations ($g_x^{(2)}$) of the drain currents. The auto-correlation function shows a clear suppression around $\tau = 0$, corresponding to the anti-bunching of electrons due to the strong Coulomb interactions on the dots, which prevent the simultaneous tunneling of electrons into the same lead. The cross-correlations, by contrast, exhibit a peak well above the uncorrelated value of one, showing how Cooper pair splitting leads to nearly simultaneous tunneling of electrons into different leads.

Information about the regularity of the dynamic Cooper pair splitter can be obtained from the waiting times between the tunneling events [19, 50]. The distribution of waiting times can be expressed as [51–55]

$$W_{\ell\ell'}(\tau) = \int_0^T dt_0 \frac{\langle\langle \mathcal{J}_\ell \mathcal{U}_\ell(t_0 + \tau, t_0) \mathcal{J}_{\ell'} \rangle\rangle_{t_0}}{\langle\langle \mathcal{J}_{\ell'} \rangle\rangle_{t_0}} P_{\ell'}(t_0), \quad (10)$$

where $\mathcal{U}_\ell(t, t_0) = \mathcal{T} \exp[\int_{t_0}^t (\mathcal{L}(\mathbf{0}, t') - \sum_\sigma \mathcal{J}_{\ell\sigma}) dt']$ is the time-evolution operator excluding electron tunneling into

drain ℓ . For $\ell = \ell'$, we obtain the distribution of waiting times between electrons tunneling into the same lead, while for $\ell \neq \ell'$, the distribution characterizes the waiting time between electrons tunneling into different leads.

Figure 3(b,c) shows both types of distributions. With a long unloading time, $\Gamma T_2 \gg 1$, electrons tunneling into the same drain tend to be separated by the period of the drive, as seen in Fig. 3(b), reflecting the regular splitting of Cooper pairs. For shorter unloading times, the dots are not always emptied in the second phase, and the Cooper pair splitting becomes less regular. This picture is corroborated by the distributions for tunneling into different leads shown in Fig. 3(c). Here, the first peak at short waiting times corresponds to the tunneling of electrons from the same split Cooper pair into different leads. In addition, the second peak corresponds to the waiting time between the last electron from one split Cooper pair and the first electron from the next split pair, and those are spaced by an interval, which is slightly shorter than the period of the drive. Again, we observe that a short unloading time reduces the regularity of the splitting.

Based on our analysis of the low-frequency noise and the time-domain statistics, we see that the dynamic Cooper pair splitter can deliver a noiseless and regular flow of split Cooper pairs that are separated by the period of the drive. These features make the dynamic Cooper pair splitter attractive for a variety of quantum information processes that require controlled generation of entanglement. The Cooper pair splitter may be operated across a wide range of driving frequencies. For example, to generate measurable currents, driving frequencies in the mega-hertz regime produce pico-ampere currents. On the other hand, slower driving speeds are suitable for single-electron detection as in the experiment of Ref. [19].

Perspectives.— We have proposed and analyzed a dynamic Cooper pair splitter that can generate a noiseless and regular flow of spin-entangled electrons, when operated under optimal conditions. Our proposals appears feasible in the light of recent experiments [19, 50], and it may thus pave the way for the controlled and pulsed

generation of spin-entangled electrons in solid-state architectures. Furthermore, entanglement witnesses based on current cross-correlations [46, 47] may be used to experimentally certify the spin-entanglement of mobile electrons emitted by a dynamic Cooper pair splitter.

Acknowledgements.— We thank N. Walldorf for his involvement at an early stage of the project and A. Ranni and V. F. Maisi for useful discussions. We acknowledge support from Aalto Science Institute and Academy of Finland through the Finnish Centre of Excellence in Quantum Technology (project numbers 312057 and 312299) and grants number 308515 and 331737.

-
- [1] M. Tinkham, *Introduction to Superconductivity* (Dover Publications, 2004).
- [2] G. B. Lesovik, T. Martin, and G. Blatter, Electronic entanglement in the vicinity of a superconductor, *Eur. Phys. J. B* **24**, 287 (2001).
- [3] P. Recher, E. V. Sukhorukov, and D. Loss, Andreev tunneling, Coulomb blockade, and resonant transport of non-local spin-entangled electrons, *Phys. Rev. B* **63**, 165314 (2001).
- [4] D. Beckmann, H. B. Weber, and H. v. Löhneysen, Evidence for Crossed Andreev Reflection in Superconductor-Ferromagnet Hybrid Structures, *Phys. Rev. Lett.* **93**, 197003 (2004).
- [5] S. Russo, M. Kroug, T. M. Klapwijk, and A. F. Morpurgo, Experimental Observation of Bias-Dependent Nonlocal Andreev Reflection, *Phys. Rev. Lett.* **95**, 027002 (2005).
- [6] L. Hofstetter, S. Csonka, J. Nygård, and C. Schönberger, Cooper pair splitter realized in a two-quantum-dot Y-junction, *Nature* **461**, 960 (2009).
- [7] L. G. Herrmann, F. Portier, P. Roche, A. L. Yeyati, T. Kontos, and C. Strunk, Carbon Nanotubes as Cooper-Pair Beam Splitters, *Phys. Rev. Lett.* **104**, 026801 (2010).
- [8] J. Wei and V. Chandrasekhar, Positive noise cross-correlation in hybrid superconducting and normal-metal three-terminal devices, *Nat. Phys.* **6**, 494 (2010).
- [9] L. Hofstetter, S. Csonka, A. Baumgartner, G. Fülöp, S. d’Hollosy, J. Nygård, and C. Schönberger, Finite-Bias Cooper Pair Splitting, *Phys. Rev. Lett.* **107**, 136801 (2011).
- [10] J. Schindele, A. Baumgartner, and C. Schönberger, Near-Unity Cooper Pair Splitting Efficiency, *Phys. Rev. Lett.* **109**, 157002 (2012).
- [11] L. G. Herrmann, P. Buset, W. J. Herrera, F. Portier, P. Roche, C. Strunk, A. Levy Yeyati, and T. Kontos, Spectroscopy of non-local superconducting correlations in a double quantum dot, [arXiv:1205.1972](https://arxiv.org/abs/1205.1972).
- [12] A. Das, R. Ronen, M. Heiblum, D. Mahalu, A. V. Kretinin, and H. Shtrikman, High-efficiency Cooper pair splitting demonstrated by two-particle conductance resonance and positive noise cross-correlation, *Nat. Commun.* **3**, 1165 (2012).
- [13] G. Fülöp, S. d’Hollosy, A. Baumgartner, P. Makk, V. A. Guzenko, M. H. Madsen, J. Nygård, C. Schönberger, and S. Csonka, Local electrical tuning of the nonlocal signals in a Cooper pair splitter, *Phys. Rev. B* **90**, 235412 (2014).
- [14] Z. B. Tan, D. Cox, T. Nieminen, P. Lähteenmäki, D. Golubev, G. B. Lesovik, and P. J. Hakonen, Cooper Pair Splitting by Means of Graphene Quantum Dots, *Phys. Rev. Lett.* **114**, 096602 (2015).
- [15] G. Fülöp, F. Domínguez, S. d’Hollosy, A. Baumgartner, P. Makk, M. H. Madsen, V. A. Guzenko, J. Nygård, C. Schönberger, A. Levy Yeyati, and S. Csonka, Magnetic field tuning and quantum interference in a Cooper pair splitter, *Phys. Rev. Lett.* **115**, 227003 (2015).
- [16] I. V. Borzenets, Y. Shimazaki, G. F. Jones, M. F. Craciun, S. Russo, M. Yamamoto, and S. Tarucha, High Efficiency CVD Graphene-lead (Pb) Cooper Pair Splitter, *Sci. Rep.* **6**, 23051 (2016).
- [17] L. E. Bruhat, T. Cubaynes, J. J. Viennot, M. C. Dartailh, M. M. Desjardins, A. Cottet, and T. Kontos, Circuit QED with a quantum-dot charge qubit dressed by Cooper pairs, *Phys. Rev. B* **98**, 155313 (2018).
- [18] Z. B. Tan, A. Laitinen, N. S. Kirsanov, A. Galda, V. M. Vinokur, M. Haque, A. Savin, D. S. Golubev, G. B. Lesovik, and P. J. Hakonen, Thermoelectric current in a graphene Cooper pair splitter, *Nat. Commun.* **12**, 138 (2021).
- [19] A. Ranni, F. Brange, E. T. Mannila, C. Flindt, and V. F. Maisi, Real-time observation of Cooper pair splitting showing strong non-local correlations, [arXiv:2012.10373](https://arxiv.org/abs/2012.10373).
- [20] G. Fève, A. Mahé, J.-M. Berroir, T. Kontos, B. Plaçais, D. C. Glattli, A. Cavanna, B. Etienne, and Y. Jin, An on-demand coherent single-electron source, *Science* **316**, 1169 (2007).
- [21] M. D. Blumenthal, B. Kaestner, L. Li, S. Giblin, T. J. B. M. Janssen, M. Pepper, D. Anderson, G. Jones, and D. A. Ritchie, Gigahertz quantized charge pumping, *Nat. Phys.* **3**, 343 (2007).
- [22] E. Bocquillon, V. Freulon, J.-M. Berroir, P. Degiovanni, B. Plaçais, A. Cavanna, Y. Jin, and G. Fève, Coherence and indistinguishability of single electrons emitted by independent sources, *Science* **339**, 1054 (2013).
- [23] J. Dubois, T. Jullien, F. Portier, P. Roche, A. Cavanna, Y. Jin, W. Wegscheider, P. Roulleau, and D. C. Glattli, Minimal-excitation states for electron quantum optics using levitons, *Nature* **502**, 659 (2013).
- [24] J. D. Fletcher, P. See, H. Howe, M. Pepper, S. P. Giblin, J. P. Griffiths, G. A. C. Jones, I. Farrer, D. A. Ritchie, T. J. B. M. Janssen, and M. Kataoka, Clock-Controlled Emission of Single-Electron Wave Packets in a Solid-State Circuit, *Phys. Rev. Lett.* **111**, 216807 (2013).
- [25] L. Fricke, M. Wulf, B. Kaestner, F. Hohls, P. Mirovsky, B. Mackrodt, R. Dolata, T. Weimann, K. Pierz, U. Siegner, and H. W. Schumacher, Self-Referenced Single-Electron Quantized Current Source, *Phys. Rev. Lett.* **112**, 226803 (2014).
- [26] T. Jullien, P. Roulleau, B. Roche, A. Cavanna, Y. Jin, and D. C. Glattli, Quantum tomography of an electron, *Nature* **514**, 603 (2014).
- [27] N. Ubbelohde, F. Hohls, V. Kashcheyevs, T. Wagner, L. Fricke, B. Kästner, K. Pierz, H. W. Schumacher, and R. J. Haug, Partitioning of on-demand electron pairs, *Nat. Nanotech.* **10**, 46 (2015).
- [28] D. M. T. van Zanten, D. M. Basko, I. M. Khaymovich, J. P. Pekola, H. Courtois, and C. B. Winkelmann, Single Quantum Level Electron Turnstile, *Phys. Rev. Lett.* **116**, 166801 (2016).

- [29] J. P. Pekola, O.-P. Saira, V. F. Maisi, A. Kemppinen, M. Möttönen, Y. A. Pashkin, and D. V. Averin, Single-electron current sources: Toward a refined definition of the ampere, *Rev. Mod. Phys.* **85**, 1421 (2013).
- [30] O. Sauret, D. Feinberg, and T. Martin, Quantum master equations for the superconductor-quantum dot entangler, *Phys. Rev. B* **70**, 245313 (2004).
- [31] J. Eldridge, M. G. Pala, M. Governale, and J. König, Superconducting proximity effect in interacting double-dot systems, *Phys. Rev. B* **82**, 184507 (2010).
- [32] B. Hiltcher, M. Governale, J. Splettstoesser, and J. König, Adiabatic pumping in a double-dot Cooper-pair beam splitter, *Phys. Rev. B* **84**, 155403 (2011).
- [33] N. Walldorf, F. Brange, C. Padurariu, and C. Flindt, Noise and full counting statistics of a Cooper pair splitter, *Phys. Rev. B* **101**, 205422 (2020).
- [34] H.-P. Breuer and F. Petruccione, *The theory of open quantum systems* (Oxford University Press, 2003).
- [35] B. L. Hazelzet, M. R. Wegewijs, T. H. Stoof, and Y. V. Nazarov, Coherent and incoherent pumping of electrons in double quantum dots, *Phys. Rev. B* **63**, 165313 (2001).
- [36] M. B. Plenio and P. L. Knight, The quantum-jump approach to dissipative dynamics in quantum optics, *Rev. Mod. Phys.* **70**, 101 (1998).
- [37] Y. Makhlin, G. Schön, and A. Shnirman, Quantum-state engineering with Josephson-junction devices, *Rev. Mod. Phys.* **73**, 357 (2001).
- [38] F. Pistolesi, Full counting statistics of a charge shuttle, *Phys. Rev. B* **69**, 245409 (2004).
- [39] M. Albert, C. Flindt, and M. Büttiker, Accuracy of the quantum capacitor as a single-electron source, *Phys. Rev. B* **82**, 041407 (2010).
- [40] E. Potanina, K. Brandner, and C. Flindt, Optimization of quantized charge pumping using full counting statistics, *Phys. Rev. B* **99**, 035437 (2019).
- [41] C. Flindt, T. Novotný, and A.-P. Jauho, Full counting statistics of nano-electromechanical systems, *EPL* **69**, 475 (2005).
- [42] C. Flindt, T. Novotný, A. Braggio, M. Sasseti, and A.-P. Jauho, Counting Statistics of Non-Markovian Quantum Stochastic Processes, *Phys. Rev. Lett.* **100**, 150601 (2008).
- [43] C. Flindt, T. Novotný, A. Braggio, and A.-P. Jauho, Counting statistics of transport through Coulomb blockade nanostructures: High-order cumulants and non-Markovian effects, *Phys. Rev. B* **82**, 155407 (2010).
- [44] S. Kawabata, Test of Bell's Inequality using the Spin Filter Effect in Ferromagnetic Semiconductor Microstructures, *J. Phys. Soc. Jap.* **70**, 1210 (2001).
- [45] O. Malkoc, C. Bergenfeldt, and P. Samuelsson, Full counting statistics of generic spin entangler with quantum dot-ferromagnet detectors, *EPL* **105**, 47013 (2014).
- [46] P. Busz, D. Tomaszewski, and J. Martinek, Spin correlation and entanglement detection in Cooper pair splitters by current measurements using magnetic detectors, *Phys. Rev. B* **96**, 064520 (2017).
- [47] F. Brange, O. Malkoc, and P. Samuelsson, Minimal Entanglement Witness from Electrical Current Correlations, *Phys. Rev. Lett.* **118**, 036804 (2017).
- [48] H. J. Carmichael, S. Singh, R. Vyas, and P. R. Rice, Photoelectron waiting times and atomic state reduction in resonance fluorescence, *Phys. Rev. A* **39**, 1200 (1989).
- [49] C. Emary, C. Pörtl, A. Carmele, J. Kabuss, A. Knorr, and T. Brandes, Bunching and antibunching in electronic transport, *Phys. Rev. B* **85**, 165417 (2012).
- [50] F. Brange, A. Schmidt, J. C. Bayer, T. Wagner, C. Flindt, and R. J. Haug, Controlled emission time statistics of a dynamic single-electron transistor, *Sci. Adv.* **7**, eabe0793 (2021).
- [51] T. Brandes, Waiting times and noise in single particle transport, *Ann. Physik* **17**, 477 (2008).
- [52] M. Albert, C. Flindt, and M. Büttiker, Distributions of Waiting Times of Dynamic Single-Electron Emitters, *Phys. Rev. Lett.* **107**, 086805 (2011).
- [53] E. Potanina and C. Flindt, Electron waiting times of a periodically driven single-electron turnstile, *Phys. Rev. B* **96**, 045420 (2017).
- [54] N. Walldorf, C. Padurariu, A.-P. Jauho, and C. Flindt, Electron Waiting Times of a Cooper Pair Splitter, *Phys. Rev. Lett.* **120**, 087701 (2018).
- [55] K. Wrześniewski and I. Weymann, Current cross-correlations and waiting time distributions in Andreev transport through Cooper pair splitters based on a triple quantum dot system, *Phys. Rev. B* **101**, 155409 (2020).